Journal of Visualized Experiments

Quantification of Subcellular Glycogen Distribution in Skeletal Muscle Fibers Using Transmission Electron Microscopy

--Manuscript Draft--

Article Type:	Invited Results Article - JoVE Produced Video
Manuscript Number:	JoVE63347R2
Full Title:	Quantification of Subcellular Glycogen Distribution in Skeletal Muscle Fibers Using Transmission Electron Microscopy
Corresponding Author:	Joachim Nielsen University of Southern Denmark: Syddansk Universitet Odense, DENMARK
Corresponding Author's Institution:	University of Southern Denmark: Syddansk Universitet
Corresponding Author E-Mail:	jnielsen@health.sdu.dk
Order of Authors:	Rasmus Jensen
	Niels Ørtenblad
	Cristiano di Benedetto
	Klaus Qvortrup
	Joachim Nielsen
Additional Information:	
Question	**Response**
Please specify the section of the submitted manuscript.	Biochemistry
Please indicate whether this article will be Standard Access or Open Access.	Standard Access ($1400)
Please indicate the **city, state/province, and country** where this article will be **filmed**. Please do not use abbreviations.	Copenhagen, Denmark
Please confirm that you have read and agree to the terms and conditions of the author license agreement that applies below:	I agree to the Author License Agreement
Please confirm that you have read and agree to the terms and conditions of the video release that applies below:	I agree to the Video Release
Please provide any comments to the journal here.	

TITLE:

Quantification of Subcellular Glycogen Distribution in Skeletal Muscle Fibers Using Transmission Electron Microscopy

AUTHORS AND AFFILIATIONS:

Rasmus Jensen[1], Niels Ørtenblad[2], Cristiano di Benedetto[3], Klaus Qvortrup[3], Joachim Nielsen[2*]

[1]Research center for applied health science, University College South Denmark, Denmark.
[2]Department of Sports Science and Clinical Biomechanics, University of Southern Denmark, Denmark.
[3]Department of Biomedical Sciences, Core Facility for Integrated Microscopy, University of Copenhagen, Denmark.

*Corresponding Author:
Joachim Nielsen (jnielsen@health.sdu.dk)

Email addresses of co-authors:
Rasmus Jensen (RJEN@ucsyd.dk)
Niels Ørtenblad (nortenblad@health.sdu.dk)
Cristiano di Benedetto (cristiano@sund.ku.dk)
Klaus Qvortrup (qvortrup@sund.ku.dk)
Joachim Nielsen (jnielsen@health.sdu.dk)

SUMMARY:

A modified post-fixation procedure increases the contrast of glycogen particles in tissue. This paper provides a step-by-step protocol describing how to handle the tissue, conduct the imaging, and use stereological methods to obtain unbiased and quantitative data on fiber type-specific subcellular glycogen distribution in skeletal muscle.

ABSTRACT:

With the use of transmission electron microscopy, high-resolution images of fixed samples containing individual muscle fibers can be obtained. This enables quantifications of ultrastructural aspects such as volume fractions, surface area to volume ratios, morphometry, and physical contact sites of different subcellular structures. In the 1970s, a protocol for enhanced staining of glycogen in cells was developed and paved the way for a string of studies on the subcellular localization of glycogen and glycogen particle size using transmission electron microscopy. While most analyses interpret glycogen as if it is homogeneously distributed within the muscle fibers, providing only a single value (e.g., an average concentration), transmission electron microscopy has revealed that glycogen is stored as discrete glycogen particles located in distinct subcellular compartments. Here, the step-by-step protocol from tissue collection to the quantitative determination of the volume fraction and particle diameter of glycogen in the distinct subcellular compartments of individual skeletal muscle fibers is described. Considerations on how to 1) collect and stain tissue specimens, 2) perform image analyses and data handling, 3) evaluate the precision of estimates, 4) discriminate between muscle fiber types,

and 5) methodological pitfalls and limitations are included.

INTRODUCTION:

Glycogen particles are composed of branched polymers of glucose and various associated proteins[1] and constitute an important fuel during high metabolic demands[2]. Although not widely recognized, glycogen particles also constitute a local fuel, where some subcellular processes preferentially utilize glycogen despite the availability of other and more long-lasting fuels as plasma glucose and fatty acids[3,4].

The importance of storing glycogen as a subcellular specific localized fuel has been discussed in several reviews[5,6] mainly based on some of the earliest documentations of the subcellular distribution of glycogen by transmission electron microscopy (TEM)[7,8]. The first studies used different protocols to increase the contrast of glycogen from histochemical staining techniques to negative and positive stainings[9,10]. An important methodological development was the refined post-fixation protocol with the potassium ferrocyanide-reduced osmium[11–14], which significantly improved the contrast of glycogen particles. This refined protocol was not used in some of the pioneering work on exercise-induced glycogen depletion[15] but was re-introduced by Graham and colleagues[16,17].

Based on the 2-dimensional images, the subcellular distribution of glycogen is most often described as glycogen particles located in three pools: subsarcolemmal (just beneath the surface membrane), intermyofibrillar (between the myofibrils), or intramyofibrillar (within the myofibrils). However, glycogen particles could also be described as associated with, for example, sarcoplasmic reticulum[7] or nuclei[18]. In addition to the subcellular distribution, the advantage of TEM-estimated glycogen content is also that quantification can be conducted at the single fiber level. This allows investigation of fiber-to-fiber variability and correlative analyses with fiber types and cellular components as mitochondria and lipid droplets.

Here, the protocol for the TEM-estimated fiber type-specific volumetric content of the three common subcellular pools of glycogen (subsarcolemmal, intermyofibrillar, and intramyofibrillar) in skeletal muscle fibers is described. The method has been applied to skeletal muscles from humans[19], rats[20], and mice[21]; as well as birds and fish[22]; and cardiomyocytes from rats[23].

PROTOCOL:

The present protocol using human biopsied skeletal muscle samples was approved by The Regional Committees on Health Research Ethics for Southern Denmark (S-20170198). Muscle biopsies were obtained through an incision in the skin from the *vastus lateralis* muscle using a Bergström needle with suction after local anesthesia was given subcutaneously (1–3 mL of Lidocaine 2% per incision). If isolated whole rat muscles were used, the animals were sacrificed by cervical dislocation before the muscle biopsies were obtained, in accordance with the guidelines of the animal ethics committee at Odense University Hospital, Denmark.

1. Primary fixation, post-fixation, embedding, sectioning, and contrasting

1.1. Prepare 1.6 mL of primary fixative solution (2.5% glutaraldehyde in 0.1 M sodium cacodylate buffer (pH 7.3)) in a 2 mL micro centrifugation tube. Store it at 5 ˚C for a maximum of 14 days.

1.2. From the muscle biopsy or whole muscle, isolate a small specimen, which has a maximum diameter of 1 mm in any direction and is a bit longer in the longitudinal fiber direction than cross-sectionally (for orientation purposes).

1.3. Place the specimen in the tube containing the cold primary fixation solution. Store it at 5 ˚C for 24 h.

1.4. Wash the specimen four times (15 min between each wash) in 0.1 M sodium cacodylate buffer (pH 7.3). Using transfer pipettes, remove the used buffer from the tube leaving the specimen untouched, and subsequently add the fresh buffer.

NOTE: Following the final wash, the specimen can be stored in the 0.1 M sodium cacodylate buffer at 5 ˚C for several months[11]. The protocol can be paused here.

1.5. Postfix with 1% osmium tetroxide (OsO_4) and 1.5% potassium ferrocyanide ($K_4Fe(CN)_6$) in 0.1 M sodium cacodylate buffer (pH 7.3) for 120 min at 4 ˚C.

NOTE: The use of 1.5% potassium ferrocyanide ($K_4Fe(CN)_6$) is essential for an optimal contrast of glycogen particles[11–13].

1.6. Rinse twice in double-distilled water at room temperature (RT).

1.7. Dehydrate by submerging in a graded series of alcohol (ethanol) at RT using the following concentrations: 70% (10 min), 70% (10 min), 95% (10 min), 100% (10 min), and 100% (10 min).

NOTE: In each step, the specimen is submerged in ethanol, which is subsequently only partly removed to avoid drying of the specimen. Finally, the left-over ethanol is discarded.

1.8. Infiltrate with graded mixtures of propylene oxide and epossidic resin at RT using the following volume ratios (propylene oxide/epossidic resin): 1/0 (10 min), 1/0 (10 min), 3/1 (45 min), 1/1 (45 min), 1/3 (45 min), 0/1 (overnight). The following day, embed specimens in 100% fresh epossidic resin in molds and polymerize at 60 ˚C for 48 h.

NOTE: This graded method is per the previous protocols[11,12]. The protocol can be paused here.

1.9. Cut ultra-thin (60–70 nm) sections of longitudinally oriented fibers and collect them on one-hole copper grids as follows.

1.9.1. Mount the block of a specimen on the ultramicrotome holder.

1.9.2. Trim the block on the surface with a razor blade in order to reach the level of the tissue.

1.9.3. Mount a diamond knife (ultracut 45) in front of the sample and align the sample surface parallel to the knife.

1.9.4. Produce a semi-thin (1 µm) section with the diamond knife to check the orientation of the sample. Stain the semi-thin section with toluidine blue for observation with light microscopy.

1.9.5. Trim the block further to reduce the area of interest in order to get proper ultrathin sections.

1.9.6. Cut ultrathin (60–70 nm) sections with a second diamond knife (ultracut 45).

1.9.7. Collect 1–2 sections on one-hole copper grids using a Perfect Loop.

NOTE: One-hole copper grid has a single hole in the middle with Formvar supporting membrane.

1.10. Contrast sections with uranyl acetate and lead citrate by immersing the above grids in uranyl acetate solution (0.5% in double-distilled water) for 20 min, and then in lead citrate solution (1% in double-distilled water) for 15 min. Wash the grids in double-distilled water between and after the two stains.

NOTE: The protocol can be paused here.

2. Imaging

2.1. Turn on the transmission electron microscope (operated at an accelerating voltage of 80 kV), computer, and image recording software. Record digital images with a digital slow-scan 2 k x 2 k CCD camera and the associated imaging software.

2.2. Insert the grid with multiple sections in the microscope stage.

2.3. Screen the grid initially at low magnification (e.g., x100) to determine the quality of sections (i.e., holes in the supporting membrane, debris, etc.) and choose the best quality sections. At low magnification, determine the direction of the muscle fibers.

2.4. Next, increase the magnification with the beam centered on a peripheral fiber in the section. Focus the image at magnification above 30 k to ensure sufficient fine details in the image, guided by a Real-Time Fast Fourier Transformation, if available. Finally, record images with 1 s exposure time at the desired magnification.

2.5. Acquire a total of 24 images of a randomly selected fiber, i.e., 12 images of the myofibrillar space and 12 images of the subsarcolemmal space, at a magnification between 10 k and 40 k. Ensure that the images are distributed across the length and width of the fiber in a randomized but systematic order to obtain unbiased results (**Figure 1A**).

NOTE: The optimal magnification depends on the available camera resolution and the size of the micrographs. The goal is to achieve a final resolution, where glycogen particle diameters can be measured within 1 nm steps, and to include a total area of the myofibrillar region of at least 70 μm^2 and a total length of the fiber of at least 25 µm distributed into 12 images of the myofibrillar space and 12 images of the subsarcolemmal space per fiber, respectively. The 24 images per fiber will most likely give a precision (coefficient of error) of the volumetric content of the different pools of glycogen between 0.1 and 0.2 in individual fibers from human, rat, and mice skeletal muscles[20,21,24] (**Figure 2E**).

2.6. Repeat steps 2.4 and 2.5 until a total of 6–10 fibers are imaged. If needed, cut additional sections (separated by at least 150 µm to avoid overlap of already imaged fibers) and repeat steps 1.9–2.5.

3. Image analyses

3.1. Import images to ImageJ by clicking on **File** > **Open**.

3.2. Set global scale to match the original size of the image by clicking on **Analyze** > **Set Scale**.

3.3. Zoom in 100% by clicking on **Image** > **Zoom** > **In**.

3.4. Measure the thickness of one Z-disc per image of the myofibrillar space (12 per fiber) using the **Straight Line** tool from the Tools menu (**Figure 1D**). Calculate the average Z-disc thickness of each of the 6–10 fibers.

3.5. Define 2–3 fibers with the thickest average Z-disc as type 1 fibers and 2–3 fibers with the thinnest average Z-disc as type 2 fibers. Disregard the intermediate 2–4 fibers for further analyses (**Figure 1E**).

NOTE: The following steps are repeated for each of the 4–6 fibers from the sample. The glycogen volume fractions are estimated by point counting as described elsewhere[25,26]. The size of the grids is chosen to obtain a satisfactory high precision of the estimates. This is often obtained by achieving 250 hits, which then dictates the total number of points needed and, in turn, the area per point.

3.6. Use the **Segmented Line** tool to measure the length of the outermost myofibril visible just below the subsarcolemmal region (**Figure 2A**).

NOTE: This length is used to express subsarcolemmal glycogen per surface area (i.e., length of the outermost myofibril multiplied by the thickness of the section (60 nm); see step 4.5). Therefore, only the subsarcolemmal region, which is represented by this length, is included in the analysis.

3.7. Insert a grid by clicking on **Analyze** > **Tools** > **Grid** and set **Area Per Point** at 32,400 nm^2. Count the number of hits within the available length in the 12 subsarcolemmal images, where a cross hits the subsarcolemmal glycogen (**Figure 2A**). A hit is defined as a glycogen particle being present in the upper-right corner of a cross.

3.8. Insert a grid by clicking on **Analyze** > **Tools** > **Grid** and set **Area Per Point** at 160,000 nm^2. Count the number of hits in the 12 myofibrillar images, where a cross hits the intramyofibrillar space (**Figure 2B**).

3.9. Insert a grid by clicking on **Analyze** > **Tools** > **Grid** and set **Area Per Point** at 3,600 nm^2. Count the number of hits in the 12 myofibrillar images, where a cross hits the intramyofibrillar glycogen (**Figure 2C**).

3.10. Insert a grid by clicking on **Analyze** > **Tools** > **Grid** and set **Area Per Point** at 32,400 nm^2. Count the number of hits in the 12 myofibrillar images, where a cross hits the intermyofibrillar glycogen (**Figure 2D**).

3.11. Using the **Straight Line** tool, measure the diameter of five randomly chosen glycogen particles of each pool for each of the 12 images to obtain an average of 60 particles per pool per fiber.

NOTE: The average of 60 particles largely covers the variation within the fiber (**Figure 2F**).

4. Calculations

4.1. Calculate the apparent area fraction (A_A) of the intramyofibrillar space per myofibrillar space as the sum of all hits divided by the sum of all points from the 12 images (from step 3.8).

4.2. Calculate the apparent area fraction of intramyofibrillar glycogen per myofibrillar area, intermyofibrillar glycogen per myofibrillar area, and subsarcolemmal glycogen per image area as the sum of all hits divided by the sum of all points from the 12 images (from steps 3.7, 3.9, and 3.10).

4.3. Calculate the volume fraction (V_V) of intramyofibrillar, intermyofibrillar, and subsarcolemmal glycogen, respectively, as the apparent area fraction (A_A) minus the product of surface density (S_V) with section thickness (t), where surface density is the numerical density of particles multiplied by the mean particle surface:

$$V_v = A_A - (1 / 4) \cdot S_v \cdot t$$

where

$$S_v\ (\mu m^{-1}) = A_A / ((\pi \cdot (((1 / 2) \cdot H)^2)) \cdot (t + H))$$

$t = 0.06\ \mu m$

H = mean diameter of the particles (µm)

NOTE: The volume fraction is smaller than the apparent area fraction due to the contribution of caps from particles with their center outside the slice[25].

4.4. To express intramyofibrillar glycogen per intramyofibrillar space, divide the area fraction of intramyofibrillar glycogen (step 4.2) by the area fraction of the intramyofibrillar space (step 4.1). The intermyofibrillar glycogen is expressed per myofibrillar space as calculated in the previous step (step 4.3).

4.5. To express subsarcolemmal glycogen per surface area of the fiber (V_S) (outermost myofibril), convert the volume fraction of glycogen to an absolute amount by multiplying with the volume of the image (product of area and section thickness) and dividing by the product of mean available length (from step 3.6) with section thickness (t).

4.6. Estimate the total volumetric glycogen content using the values from steps 4.1, 4.4, and 4.5, as follows:

Myofibrillar glycogen = Intermyofibrillar glycogen + (intramyofibrillar glycogen · area fraction of intramyofibrillar space)

By assuming an average fiber radius of 40 μm[27], the volume to surface ratio is 20:1, so total glycogen is:

Total glycogen (V_V) = Myofibrillar glycogen + (subsarcolemmal glycogen (V_S) / 20)

NOTE: The volume to surface ratio of 20:1 can vary from fiber to fiber depending on the actual fiber size and the size of the subsarcolemmal region. This is not taken into account with the present protocol.

4.7. From this, the relative contribution from each pool is calculated as fractions of total glycogen:

Intermyofibrillar glycogen / Total glycogen
= Intermyofibrillar glycogen / Total glycogen

Intramyofibrillar glycogen / Total glycogen
= (Intramyofibrillar glycogen · area fraction of intramyofibrillar space) / Total glycogen

Subsarcolemmal glycogen / Total glycogen
= Subsarcolemmal glycogen / 20 / Total glycogen

4.8. For each glycogen pool, calculate the coefficient of error (CE), which expresses the uncertainty of the glycogen estimate on a fiber level, based on the number of images (n), the total number of crosses in each image (x), and the number of crosses hitting glycogen in the relevant pool in each image (y) as follows[28]:

$$CE = n^{-1} \cdot \sum x^2 \cdot (\sum x)^{-2} + \sum y^2 \cdot (\sum y)^{-2} - 2\sum (xy) \cdot \sum x^{-1} \cdot \sum y^{-1}$$

REPRESENTATIVE RESULTS:

Using this protocol, glycogen particles appear black and distinct (**Figures 1** and **Figure 2**). The normal values of glycogen are depicted in **Figure 3**. These data are based on a total of 362 fibers from 41 healthy young men as collected in different previous studies[19,24,29–31]. Here, it can be seen that intermyofibrillar glycogen values are distributed close to normal, whereas both intramyofibrillar and subsarcolemmal glycogen show a skewed distribution, where fibers sometimes have an excessive amount of glycogen. It is important to note that in normal-sized muscle fiber (diameter of 60–80 μm), intermyofibrillar glycogen is the largest pool constituting around 80% of total glycogen content. Intramyofibrillar and subsarcolemmal glycogen each constitute around 10% of the total content.

FIGURE AND TABLE LEGENDS:

Figure 1: Imaging and fiber typing. (**A**) Each fiber is imaged in a randomized systematic order. (**B**) Example of an image from the subsarcolemmal space. (**C**) Example of an image from the myofibrillar space. (**D**) In each myofibrillar image, the width of one Z-disc is measured (red lines). The measurements of a total of 12 Z-discs (one per image) give a coefficient of error of approximately 0.03. (**E**) The typical distribution of the average fiber Z-disc width in 6–10 fibers of each of the 10 biopsies. From each biopsy, 2–3 fibers are defined as types 1 and 2 based on the within-biopsy distribution. The images originate from a biopsy of *m. vastus lateralis* of a powerlifter included in a previous study[29]. m: mitochondria and Z: Z-disc.

Figure 2: Glycogen analyses. (**A**) Subsarcolemmal glycogen volume per surface area is estimated by point counting using a grid size of 180 nm x 180 nm within a region defined by the length of the outermost myofibril and the subsarcolemmal region perpendicular to this length (blue dotted lines). (**B**) The myofibrillar volume fraction is estimated by point counting using a grid size of 400 nm x 400 nm. (**C**) The volume fraction of intramyofibrillar glycogen is estimated by point counting using a grid size of 60 nm x 60 nm. (**D**) The volume fraction of intermyofibrillar glycogen is estimated by point counting using a grid size of 180 nm x 180 nm. In **A–D**, the red circles indicate hits (a cross that hits a glycogen particle). (**E**) The estimated coefficient of error for a stereological ratio estimate[24] for 2 to 12 analyzed images. The coefficient of error is estimated based on the number of counts and therefore varies between samples based on the glycogen concentration. It is often relatively low when the glycogen content is high and vice versa. (**F**) The coefficient of variation of glycogen particle diameter after measuring 2–99 particles.

Figure 3: Normal values of the three subcellular pools of glycogen in skeletal muscle. The violin plots are based on 362 fibers from 41 healthy young men (18–39 years old). The fibers originate from previous studies, wherein biopsies from *m. vastus lateralis* in a resting or control condition were obtained[19,24,29–31]. Values are shown as a box plot with a marker for the median and a box indicating the interquartile range. The lines represent upper and lower adjacent values. The boxes are overlaid by kernel density plots.

DISCUSSION:

The critical step of the method is the use of reduced osmium by potassium ferrocyanide during post-fixation. The selectivity of this modified fixative for glycogen detection cannot be fully explained by chemistry, but also includes experimental findings demonstrating no detection of such particles in tissues known to be free of glycogen or in the extracellular space[11].

Critical parameters are the precision of the estimates and the fiber-to-fiber variation. By following the present protocol for imaging, a coefficient of error between 0.1 and 0.2 of the estimates of the different pools of glycogen per fiber is obtained. This level of error is well below the variation between individual fibers (**Figure 3**). It is encouraged to report such precision estimates when estimating the volumetric content of glycogen. The presented fiber typing method is validated against myosin ATPase isoform[29]. The Z-disc thickness and mitochondrial volume fraction can also be used in combination to indicate fiber type, but not mitochondrial volume fraction alone[32].

The major limitations of the method are the inability to detect the very small glycogen particles and that profiles of glycogen particles may overlap in the projected image[28]. The first limitation invalidates a true measure of the average particle size. This becomes a severe bias when the glycogen particles are being degraded during high metabolic demands, whereas the bias may be insignificant when the glycogen particles grow from medium to a larger size during glycogen resynthesis or super-compensation. While this may have huge implications for the estimate of average glycogen particle size at low glycogen levels, the estimates of volumetric glycogen concentrations are robust, since small, unobserved glycogen particles contribute very little toward the total glycogen content. The second limitation originates from the condition, where the glycogen particles are much smaller than the thickness of the sections. This bias is mostly present at very high glycogen concentrations and could be investigated by comparing the glycogen volume fractions of sections with different thicknesses. If a thicker section is not paralleled by a high glycogen volume fraction, it must be due to an underestimation due to more overlapping particles in the thickest section. In previous studies, the glycogen volume fraction correlates with the glycogen concentration within the range from 50 to 600 mmol kg dw^{-1} indicating no pronounced overlapping of particles. However, if the glycogen concentration increases above this level, there is no increase in intermyofibrillar glycogen indicating overlap[33]. This can be solved by extrapolating the relationship between the glycogen volume fraction and the concentration at the lower glycogen concentrations.

Based on the nm resolution provided by TEM, this protocol is at present the only method to estimate the subcellular distribution of glycogen. In addition, the methodology also permits a large-scale quantitative approach (as described here), where quantitative values can be obtained at the single fiber level. This is of immense importance in skeletal muscles with high heterogeneity in fiber recruitment during various types of exercise[2], where glycogen-dependent fatigue mechanisms only occur in some fibers. The method also has potential for other excitable tissues as cardiomyocytes, where glycogen is known to be essential for normal heart function and critical during ischemia[23,34].

ACKNOWLEDGMENTS:

This work was supported by the Swedish Olympic Committee.

DISCLOSURES:

The authors declare no competing interests.

REFERENCES:

1. Prats, C., Graham, T. E., Shearer, J. The dynamic life of the glycogen granule. *Journal of Biological Chemistry*. **293** (19), 7089–7098 (2018).
2. Gollnick, P. D., Piehl, K., Saltin, B. Selective glycogen depletion pattern in human muscle fibres after exercise of varying intensity and at varying pedalling rates. *Journal of Physiology*. **241** (1), 45–57 (1974).
3. James, J. H. et al. Stimulation of both aerobic glycolysis and Na+-K+-ATPase activity in skeletal muscle by epinephrine or amylin. *American Journal of Physiology Endocrinology Metabolism*. **277** (1), E176–E186 (1999).
4. Jensen, R., Nielsen, J., Ørtenblad, N. Inhibition of glycogenolysis prolongs action potential repriming period and impairs muscle function in rat skeletal muscle. *Journal of Physiology*. **598** (4), 789–803 (2020).
5. Green, H. J. How important is endogenous muscle glycogen to fatigue in prolonged exercise? *Canadian Journal of Physiology and Pharmacology*. **69** (2), 290–297 (1991).
6. Fitts, R. H. Cellular mechanisms of muscle fatigue. *Physiological Reviews*. **74** (1), 49–94 (1994).
7. Wanson, J. C., Drochmans, P. Role of the sarcoplasmic reticulum in glycogen metabolism. *Journal of Cellular Biology*. **54** (2), 206–224 (1972).
8. Schmalbruch H, Kamieniecka Z. Fiber types in the human brachial biceps muscle. *Experimental Neurology*. **44** (2), 313–328 (1974).
9. Drochmans, P. Morphology of glycogen. Electron microscopic study of the negative stains of particulate glycogen. *Journal of Ultrastructure Research*. **6**, 141–163 (1962).
10. Thiery, J.-P. Demonstration of polysaccharides on thin sections by electron microscopy. *Journal of Microscopy*. **6**, 987–1018 (1967).
11. De Bruijn, W. C. Glycogen, its chemistry and morphologic appearance in the electron microscope. I. A modified OsO_4 fixative which selectively contrasts glycogen. *Journal of Ultrastructural Research*. **42** (1), 29–50 (1973).
12. Robinson, J. M., Karnovsky, M. L., Karnovsky, M. J. Glycogen accumulation in polymorphonuclear leukocytes, and other intracellular alterations that occur during inflammation. *The Journal of Cell Biology*. **95** (3), 933–942 (1982).
13. Rybicka, K. K. Glycosomes – the organelles of glycogen metabolism. *Tissue and Cell*. **28** (3), 253–265 (1996).
14. Gadisseux, J. F., Evrard, P. Glial-neuronal relationship in the developing central nervous system. A histochemical-electron microscope study of radial glial cell particulate glycogen in normal and reeler mice and the human fetus. *Developmental Neuroscience*. **7** (1), 12–32 (1985).
15. Fridén, J., Seger, J., Ekblom, B. Implementation of periodic acid-thiosemicarbazide-silver proteinate staining for ultrastructural assessment of muscle glycogen utilization during

exercise. *Cell Tissue Research*. **242** (1), 229–232 (1985).
16. Marchand, I. et al. Quantification of subcellular glycogen in resting human muscle: granule size, number, and location. *Journal of Applied Physiology*. **93** (5), 1598–1607 (2002).
17. Marchand, I. et al. Quantitative assessment of human muscle glycogen granules size and number in subcellular locations during recovery from prolonged exercise. *Journal of Physiology*. **580** (Pt. 2), 617–628 (2007).
18. Sun, R. C. et al. Nuclear Glycogenolysis Modulates Histone Acetylation in Human Non-Small Cell Lung Cancers. *Cell Metabolism*. **30** (5), 903–916.e7 (2019).
19. Jensen, R. et al. Heterogeneity in subcellular muscle glycogen utilisation during exercise impacts endurance capacity in men. *Journal of Physiology*. **598** (19), 4271–4292 (2020).
20. Nielsen, J., Schrøder, H. D., Rix, C. G., Ørtenblad, N. Distinct effects of subcellular glycogen localization on tetanic relaxation time and endurance in mechanically skinned rat skeletal muscle fibres. *Journal of Physiology*. **587** (14), 3679–3690 (2009).
21. Nielsen, J., Cheng, A. J., Ørtenblad, N., Westerblad, H. Subcellular distribution of glycogen and decreased tetanic Ca2+ in fatigued single intact mouse muscle fibres. *Journal of Physiology*. **592** (9), 2003–2012 (2014).
22. Mead, A. F. et al. Fundamental constraints in synchronous muscle limit superfast motor control in vertebrates. *eLife*. **6**, e29425 (2017).
23. Nielsen, J., Johnsen, J., Pryds, K., Ørtenblad, N., Bøtker, H. E. Myocardial subcellular glycogen distribution and sarcoplasmic reticulum Ca^{2+} handling: effects of ischaemia, reperfusion and ischaemic preconditioning. *Journal of Muscle Research and Cellular Motility*. **42** (1), 17–31 (2021).
24. Nielsen, J., Holmberg, H. C., Schrøder, H. D., Saltin, B., Ørtenblad, N. Human skeletal muscle glycogen utilization in exhaustive exercise: role of subcellular localization and fibre type. *Journal of Physiology*. **589** (11), 2871–2885 (2011).
25. Weibel, E. R. Stereological Methods. Vol. 2: Theoretical Foundations. Academic Press, London (1980).
26. Gundersen, H. J. et al. Some new, simple and efficient stereological methods and their use in pathological research and diagnosis. *APMIS*. **96** (5), 379–394 (1988).
27. Saltin, B., Gollnick, P. D. Skeletal muscle adaptability: significance for metabolism and performance. In: *Handbook of Physiology. Skeletal Muscle.* Bethesda, MD: American Physiological Society. **10**, 555–632 (1983).
28. Howard, C. V., Reed, M. G. *Unbiased Stereology. Three-dimensional Measurement in Microscopy*. Bios Scientific Publishers, Oxford (2005).
29. Nielsen, J. et al. Subcellular localization-dependent decrements in skeletal muscle glycogen and mitochondria content following short-term disuse in young and old men. *American Journal of Physiology Endocrinology Metabolism*. **299** (6), E1053–E1060 (2010).
30. Hokken, R. et al. Subcellular localization- and fibre type-dependent utilization of muscle glycogen during heavy resistance exercise in elite power and Olympic weightlifters. *Acta Physiologica (Oxford)*. **231** (2), e13561 (2021).
31. Nielsen, J., Farup, J., Rahbek, S. K., de Paoli, F. V., Vissing, K. Enhanced glycogen storage of a subcellular hot spot in human skeletal muscle during early recovery from eccentric contractions. *PLoS One*. **10** (5), e0127808 (2015).
32. Sjöström, M. et al. Morphometric analyses of human muscle fiber types. *Muscle Nerve*. **5** (7**)**,

538–553 (1982).
33. Gejl, K. D. et al. Local depletion of glycogen with supramaximal exercise in human skeletal muscle fibres. *Journal of Physiology*. **595** (9), 2809–2821 (2017).
34. Stanley, W. C., Recchia, F. A., Lopaschuk, G. D. Myocardial substrate metabolism in the normal and failing heart. *Physiological Reviews*. **85** (3), 1093–1129 (2005).

Figure 1

Click here to access/download;Figure;fig 1 v10.jpg

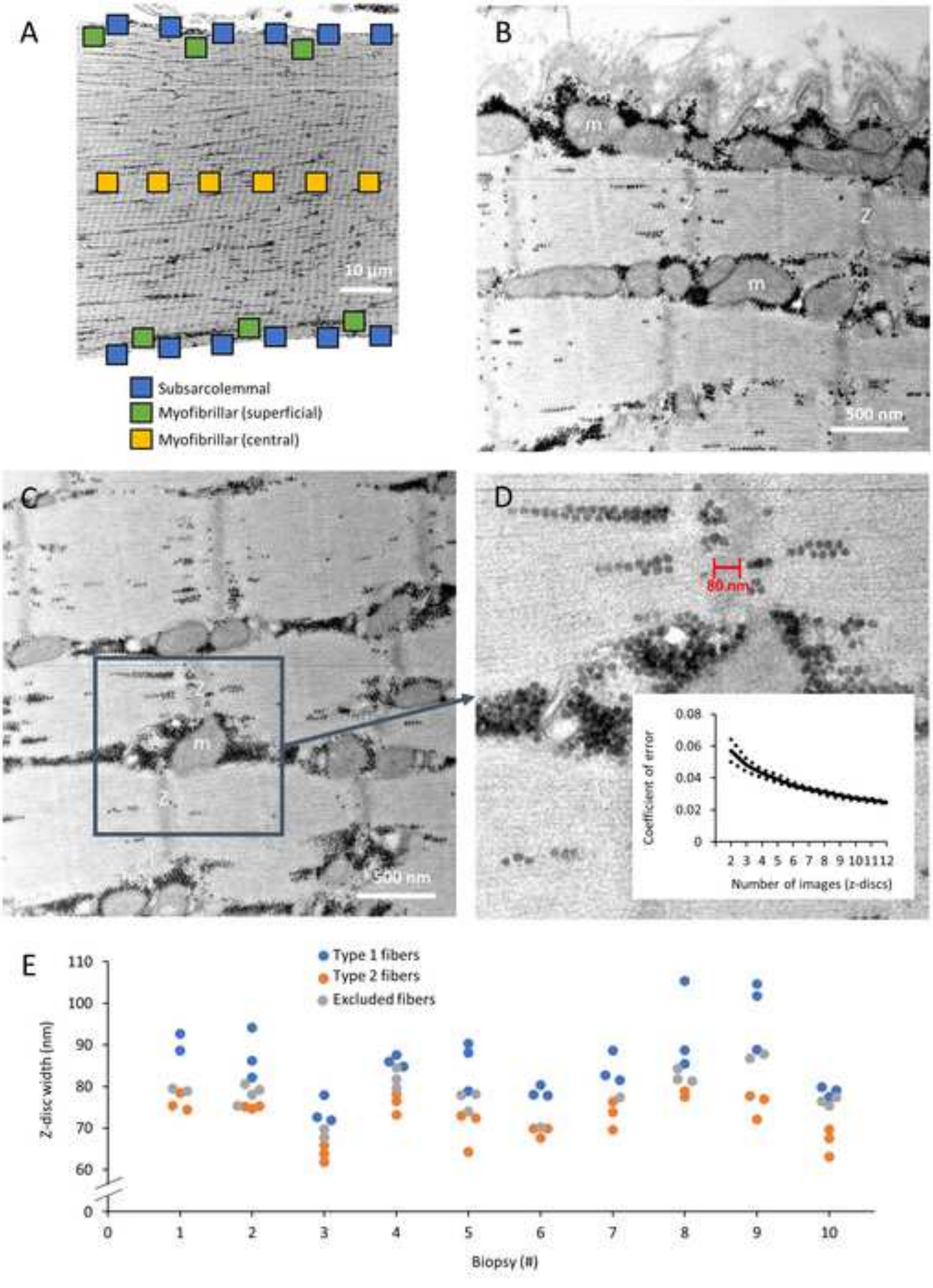

Figure 2

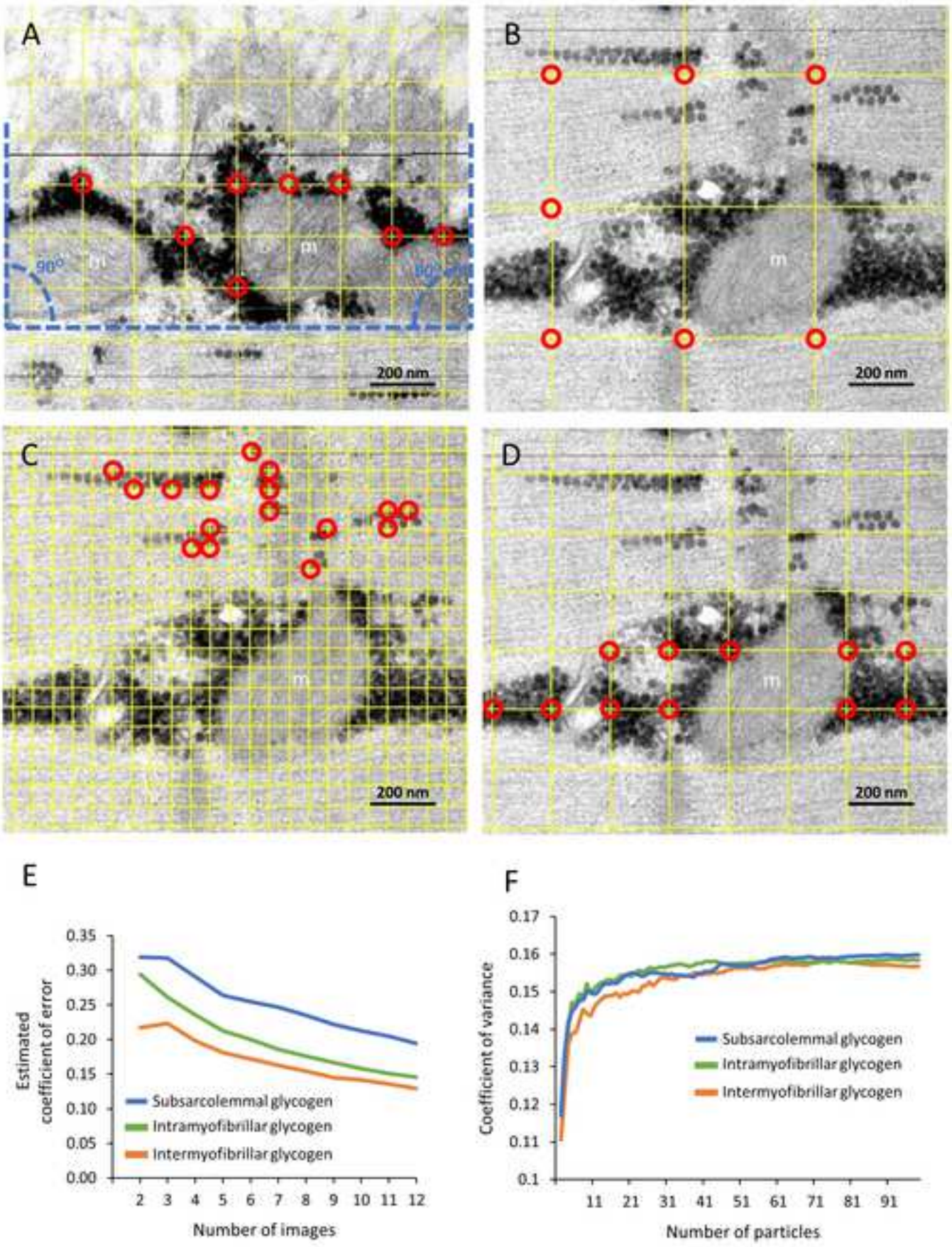

Figure 3

Click here to access/download;Figure;fig 3 results jove v02.jpg

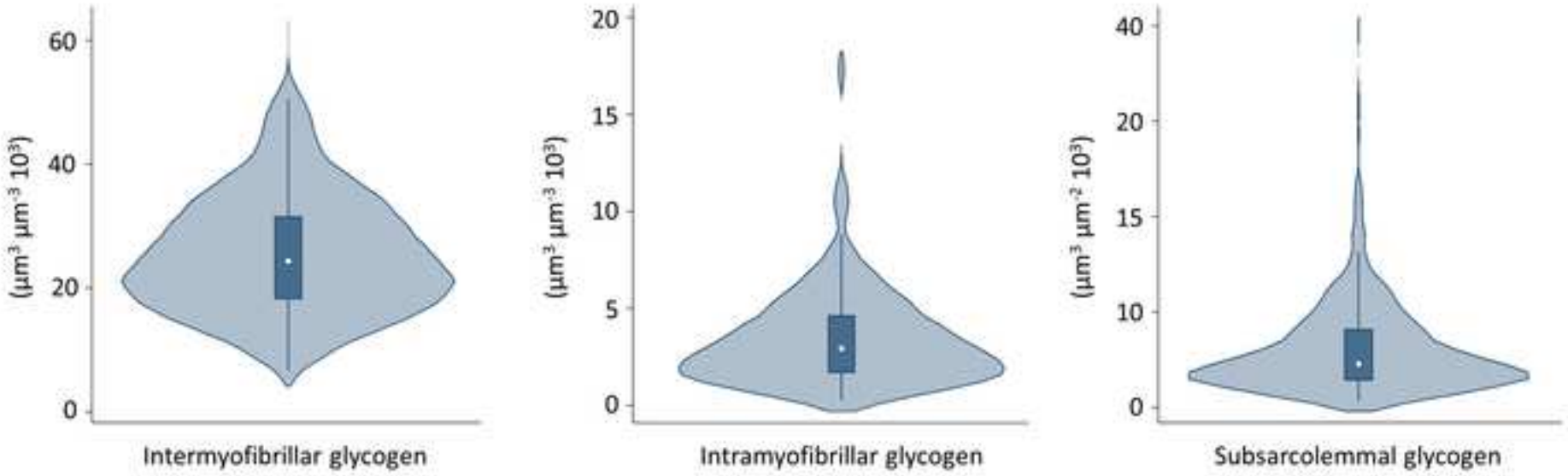

Click here to access/download

Table of Materials

Table JoVE_Materials filled v02.xls

Reply to reviewers

We thank the reviewers for their effort and insightful comments. Below we have addressed the comments point by point. Further we have uploaded a manuscript with changes highlighted.

Editorial comments:
Changes to be made by the Author(s):

1. Please take this opportunity to thoroughly proofread the manuscript to ensure that there are no spelling or grammar issues.

We have thoroughly proofread the manuscript

2. Please revise the text to avoid the use of any personal pronouns (e.g., "we", "you", "our" etc.).

The text has now been amended

3. JoVE cannot publish manuscripts containing commercial language. This includes trademark symbols (™), registered symbols (®), and company names before an instrument or reagent. Please remove all commercial language from your manuscript and use generic terms instead. All commercial products should be sufficiently referenced in the Table of Materials.
For example: Ultra-microtome Leica UC7, Leica, Wienna, Austria, Philips CM 100 Transmission EM (Philips, Eindhoven, The Netherlands, OSIS Veleta, etc.

The text has now been amended

4. Please note that your protocol will be used to generate the script for the video and must contain everything that you would like shown in the video. Please ensure you answer the "how" question, i.e., how is the step performed? Alternatively, add references to published material specifying how to perform the protocol action. There should be enough detail in each step to supplement the actions seen in the video so that viewers can easily replicate the protocol.

The text has now been amended. See also point 6-10 below.

5. Please add more details to your protocol steps:
Step 1.2: Please provide the source of the muscle samples. Please provide an ethics statement (if needed) for working with these samples.

The following paragraph has been added on page 2:

"The present protocol using human biopsied skeletal muscle samples was approved by The Regional Committees on Health Research Ethics for Southern Denmark (S-20170198). Muscle biopsies were obtained through an incision in the skin from the lateral vastus muscle using a Bergström needle with suction after local anesthesia was given subcutaneously (1–3 ml of Lidocaine 2% per incision). If isolated whole rat muscles were used, the animals were sacrificed by cervical dislocation before the muscle biopsies were

obtained, in accordance with the guidelines of the animal ethics committee at Odense University Hospital, Denmark."

6. Step 1.6, 1.7: What are the various concentrations used for graded alcohol and propylene oxide? How were these determined/selected? Please mention.

For dehydration through a graded series of alcohol (ethanol) the following concentrations were used: 70% (10 min), 70% (10 min), 95% (10 min), 100% (10 min) and 100% (10 min). The graded mixtures of propylene oxide and epossidic resim were (propylene oxide/epossidic resin): 1/0 (10 min), 1/0 (10 min), 3/1 (45 min), 1/1 (45 min), 1/3 (45 min), 0/1 (overnight). The day after, embed in 100% fresh epossidic resin at 60°C for 48h. These details have been added to section 1.6 and 1.7. The protocol is based on work by De Bruijn (1973) and Robinson et al. (1982).

7. Step 1.7: What is Epon? Is it a commercial name? If yes, please remove it from the text and use a generic term instead. Please provide details in the Table of Materials. How was embedding in Epon done?

Epon is not a commercial name, but a more precise generic term is epossidic resin. We have described it in more detail in step 1.7 and added it to the Table of materials.

8. Step 1.8: How was the sectioning setup assembled? How was the sectioning done? Please provide all associated steps.

Step 1.8 has been expanded with substeps 1.8.1 to 1.8.7, which explains all the associated steps.

9. Step 1.9: How was the contrast of the sections done? Please provide all associated steps.

Step 1.9 has been expanded with more details.

10. Step 2.4: Magnification is 10x and 40x? What does the kx stand for? How were the images acquired? Please provide all the settings and parameters used for imaging. Please mention all the steps that are necessary to execute the action item. Please provide details so a reader may replicate your analysis, including buttons clicked, inputs, screenshots, etc. Please remember that software steps without a graphical user interface (GUI) cannot be filmed.

The kx is total magnification divided by thousand. We have changed it to 10k and 40k. We have expanded step 2.3 and an extra added step (new step 2.4) to provide information about all steps. We have not described software steps, because this will be specific for the software used.

11. Step 3: Please format the commands/clicks to Analyze > Tools > Grid to emphasize the commands/options (bold letters with capitalized initial letters).

This has now been amended.

12. Please obtain explicit copyright permission to reuse any figures from a previous publication. Explicit permission can be expressed in the form of a letter from the editor or a link to the editorial policy that allows re-prints. Please upload this information as a .doc or .docx file to your Editorial Manager account. The Figure must be cited appropriately in the Figure Legend, i.e. "This figure has been modified from [citation]."

No figures are reused from a previous publication.

13. Figure 1: Please include a short description of the symbols presented in the figure in the legends.

Thanks, done.

14. Figure 3: Please describe the x/y axes.

We have re-ordered the figure, so the axes are clearly described.

15. Please ensure that the Table of Materials includes all the supplies (reagents, chemicals, instruments, equipment, software, etc.) used in the study.

Yes

16. Please do not abbreviate journal names in References.

This has now been amended.

Reviewers' comments:

Reviewer #1:

Manuscript Summary:

The ms describes a method for quantitative assessment of localized glycogen in skeletal muscle using electron microscopy images. The technique is very useful for the field of exercise and skeletal muscle, and probably in relation to myopathies and other conditions in muscle.

Major Concerns:

NA

Minor Concerns:

Protocol phase 1 certainly requires experience with histology. Slightly more detail may be required.

However, the video may cover this without the need for change.
Some typos and poor grammar, especially in Discussion.

We have added more details to the protocol as suggested by the editor (see above). We have also thoroughly proofread the manuscript.

Reviewer #2:
Manuscript Summary:
Authors describe a novel pipeline, based on an improved staining method, to quantify muscle fibers glycogen. The protocol is synthetic, concise, and straightforward to follow, from sample preparation to image acquisition and analysis. Authors complement the paper by presenting results from their own sample.

Major Concerns:
Despite the title, it is not very clear how the staining protocol differs from previous literature showing glycogen in skeletal muscle. I suspect authors took inspiration from protocols to stain brain tissue since I am guessing the "magic touch" comes from the use of reduced osmium, which is a common practice in those kinds of samples. Authors should be more clear in that sense (novelty compared to relevant literature and affine techniques), also citing relevant literature.

Thank you for bringing this to our attention. In the second paragraph of the introduction we address the historical development of the protocol. We have added a sentence about the initial protocols to highlight that the highest contrast was achieved with reduced-osmium. We agree that using reduced osmium is a common practice in ultrastructural analyses of brain tissue and have added a citation to one article within this research area. Glycogen staining in brain tissue is also based on the work by De Bruijn (1973), which we cite in the introduction.

Minor Concerns:
point 2. Imaging. Seems pretty obvious, at 2.1 "turn on the microscope". I would rather be more specific on vulgate, magnification, pixel size.

We have added more details to the protocol as suggested by the editor (see above).

Reviewer #3:
Manuscript Summary:
Glycogen is an easily accessible source of energy for various metabolic processes in many mammalian organs and tissues. Its content is especially high in skeletal muscles, where it is stored in the form of special granules (β-particles). The manuscript focuses on a quantitative method for studying of glycogen in skeletal muscles using transmission electron microscopy. The great advantage of electron microscopy is that it makes it possible to study glycogen directly in cells and tissues, and also allows information on the geometric parameters of glycogen particles. The authors modified a standard technique and described it very detailed and understandable. It is valuable that the developed protocol can be used for

the research of glycogen from skeletal muscles of various species. The method allows to obtaining of new quantitative data on glycogen particles and the peculiarities of their intracellular localization, which is certainly of fundamental and practical importance.

Minor Concerns:

1) Line 42: The authors write: "glycogen particles are branched polymers of glucose …". However, it has long been known that, in addition to the polysaccharide component represented by glucose residues connected with α-(1→4) and α-(1→6) glycosidic bonds, glycogen particles contain numerous proteins directly involved in the attachment or detachment of glucose residues or performing a regulatory function. Maybe it's worth mentioning this?

We agree that this is worth mentioning. We have added "... and associated proteins" in the first sentence of the introduction and cite Prats et al. 2018.

2) Line 109: The correct is "copper grids" not "cobber grids".

This has now been amended.

3) Lines 152, 166, and 183: The correct is "straight" not "straight".

This has now been amended.

4) Lines 191, 194, 199, and 209: "Apparent" should be replaced with "apparent".

This has now been amended.

5) Line 216: The correct is "absolute", not "absolute".

This has now been amended.

6) Line 228: The verb "is" is unnecessary.

Thanks. "is" has been changed to "each".

7) Line 300: should be replaced "or" with "of".

This has now been amended.

8) Figure 1: The scale bars are poorly visible.

We agree and have increased the font size and the thickness of the scale bars.

9) Figure 3: In the first two violin plots, the designations are μm^3 $\mu m^{-3} 10^3$, and in the third is μm^3 μm^{-2}

10^2. Looks like a mistake (typo). Indeed, in fact, all three violin plots demonstrate glycogen in different areas and the dimension should be the same. Or not?

All three subfractions are glycogen volume, but subsarcolemmal glycogen is expressed per surface area. However, it is a typo that subsarcolemmal glycogen is multiplied by 10^2, which should be 10^3.

10) How accurately was it possible to "separate" one particle from another when measuring their quantity and diameter in areas of mass accumulation of glycogen?

The mass accumulation of glycogen particles is a potential major limitation when measuring the quantity. However, as we address in the discussion (4^{th} paragraph), the underestimation of glycogen due to overlapping particles seems to be minimal within the range of glycogen concentration from 50 to 600 mmol. In clusters of particles, it is possible to measure the diameter of several of the particles. We have not investigated if the measurement of the diameter of particles in clusters is less accurate than of particles not located in clusters.